InP based Colliding Pulse Mode Locked Laser Synchronized by Electrical Subharmonic Hybrid Mode Locking

C. Ji., N. Chubun, R. Broeke, Y. Du, J. Cao, P. Bjeletich, S. J. B. Yoo
Department of Electrical and Computer Engineering, University of California, Davis, CA 95616, USA
Email: yoo@ece.ucdavis.edu
K.-Y. Liou, J. R. Lothian, and W.S.Hobson
Multiplex, Inc., 5000 Hadley Road, South Plainfield, New Jersey 07080 USA

Abstract: We report electrical subharmonic hybrid mode locking of an InP colliding pulse mode locked laser emitting low-jitter, nearly transform-limited 1.26 ps output pulses at 28 GHz with optimized RF and DC biasing conditions.

OCIS codes: 140.5960 Semiconductor lasers 140.4050 Mode-locked lasers

1. Introduction

Semiconductor mode locked lasers are ideal candidates for compact and low-cost picosecond light sources, with a wide range of applications in optical communications including ultrafast data processing, optical time-division-multiplexed (OTDM) transmission, and integrated photonic systems. Hybrid mode locking through either electrical modulation [1-3] or optical injection [4] has been investigated for eliminating the large timing jitter associated with passively mode locked lasers. Furthermore, the electrical subharmonic hybrid mode locking technique [3] allowed efficient synchronization with a lower bandwidth drive source without requiring dedicated optical setups associated with the optical injection approach [4].

Colliding Pulse Mode Locked Lasers (CPM) offer many advantages compared to other mode locked lasers providing relatively stable and better pulse-shaped mode-locking operation [1,2,4]. In this paper, we report for the first time the electrical subharmonic hybrid mode-locking (SHML) of a 3000 μm buried heterostructure (BH) CPM laser fabricated through a single step MOVPE regrowth process with nearly transform-limited output. Mode locking characteristics with respect to RF and DC biasing conditions are investigated in detail.

2. Material Composition and Device Fabrication

The CPM laser fabrication was based on a metal-organic vapor phase epitaxy (MOVPE) grown MQW structure, consisting of a 2 μm thick *p-type* InP upper cladding layer with a 0.1 μm InGaAs contact layer on top, a six quantum well active region, an undoped 0.5 μm thick InGaAsP waveguiding layer (1.15Q) directly below the active region, and a 1.5 μm thick *n-type* InP lower cladding layer. The active region consists of six 6 nm wide $In_{0.53}Ga_{0.47}As$ quantum wells separated by 7 nm wide InGaAsP (1.25Q) barriers. The lasing wavelength was slightly shifted to 1.58 μm unintentionally from the intended 1.55 μm during the material growth. The eventual goal was to integrate the CPM laser active sections with passive waveguides for extending the cavity length and minimizing the drive current requirements, and ultimately integrating CPM lasers with passive routing waveguides connecting to other optical components for realizing monolithically integrated chip-scale subsystems [5]. The 0.5 μm waveguiding layer below the active region was designed to be continuous across the active-passive interface, allowing the waveguide mode to propagate through the interface with minimal coupling loss and back-reflection.

The CPM device fabrication started with the waveguide definition. A 2500 Å thick PECVD grown SiO_2 layer was patterned by Reactive Ion Etching (RIE) to provide the waveguide mask pattern. A methane-hydrogen based process deep etched the waveguide ridge past the 1.15Q waveguiding layer, A Fe-doped InP layer with thickness >2 μm was subsequently regrown by MOVPE, covering the dry etched waveguide sidewall and creating a BH waveguide. The rest of the process followed the standard *p*-metal deposition, sample lapping, backside *n*-metal deposition, and rapid thermal annealing. Finally, the InGaAs cap layer between the gain and saturable absorber (SA) sections was removed, resulting in electrical isolation of approximately 8 kohm between the gain and the SA sections for a 4 μm wide waveguide across the 15 μm gap. Fig. 1(a) shows the waveguide cross-section of the fabricated device, while Fig.1(b) shows the device top view with the gain and SA regions indicated. The waveguide formation through the combination of deep RIE dry etching and MOVPE regrowth creates a BH waveguide in a single regrowth step, and simultaneously providing device passivation, electrical insulation and surface planarization.

3. Device Characterization

For device characterizations, the laser bars were soldered onto a temperature controlled heaksink. DC needle-probes forward biased the gain sections of the laser. A Ground-Signal-Ground (GSG) microwave probe provided RF modulation and DC biasing to the saturable absorber (SA) section, with the DC biasing voltage combined with the RF signal through a biasing Tee. The signal tip of the GSG probe contacted the SA, while the ground tips grounded the *p-side* contacts of the gain sections. The back *n-side* of the chip was left electrically floating in this configuration. The CPM laser output coupled into a lensed fiber, passed through a fiber based optical isolator, and routed to various testing instruments, including a 40 GHz PIN detector combined with a 40 GHz RF spectrum analyzer for electrical power spectrum measurements, Optical Spectrum Analyzer for optical spectrum monitoring, and after amplification with a L-band EDFA, into a 50 GHz digital sampling scope and second harmonic generation (SHG) based autocorrelator for time domain measurements.

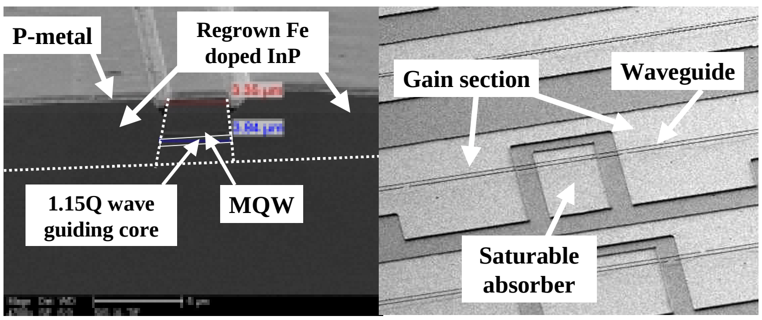

Fig. 1(a) SEM cross-sectional view of the BH waveguide.
(b) top view showing gain and SA sections of the CPM laser.

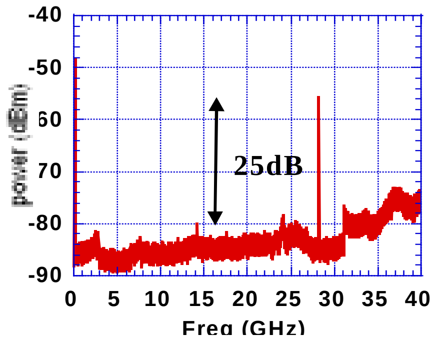

Fig. 2. RF power spectrum of a 3000 μm CPM laser under second order Subharmonic Hybrid Mode Locking (20 dBm RF power)

The experiment focused on characterizing a 3000 μm-long CPM laser including a 50 μm-long SA section and 15 μm gaps between the gain and SA sections. Fig. 2 shows the RF power spectrum of the CPM output with the gain sections forward biased at 150 mA, the SA section reverse biased at –4.5V and modulated with a 20 dBm second order electrical subharmonic signal. A sharp spectral peak can be observed at the CPM frequency of 28.14 GHz. The laser response at the subharmonic modulation frequency of 14.07 GHz was 25 dB lower, demonstrating minimal AM distortion [3]. With only the DC biasing applied, the laser operated in the passively mode locking regime with a relatively broad CPM spectral peak (3dB bandwidth around 1 MHz). The pulse width was nearly transform limited at 5.74 ps, with a time-bandwidth product of 0.48. Under subharmonic hybrid mode locking, the CPM spectral peak narrowed dramatically with a 3dB bandwidth of 20 kHz. This indicated that the timing jitter inherent in passively mode locking operation has been significantly reduced, and the CPM output was well synchronized to the drive signal, demonstrating the SHML as a viable technique for phase locking the CPM output to an external clock source in system level application.

We then carefully optimized the pulse width by adjusting RF and DC biasing conditions in sequence, while monitoring pulse shapes on the second harmonic autocorrelator, optical emission spectra on the optical spectrum analyzer, and pulse trains on the digital sampling scope. Fig. 3(a) shows effects of variation in RF modulation power and frequency on pulse width under above-mentioned DC biasing conditions. The pulse width exhibited a clear minimum close to the passively mode locking frequency of 28.14 GHz. The locking bandwidth also broadened and the pulse width reduced with increasing subharmonic RF power before saturating at 24 dBm RF power with a pulse width of 1.9 ps. With the RF biasing point held at a fixed 24 dBm RF signal at subharmonic modulation frequency of 14.075 GHz, Fig. 3(b) shows the effects of variations in the gain and SA DC biasing level. The pulse width reduces as the reverse bias voltage increases and the biasing current reduces. This provides more complete SA carrier sweepout, correspondingly faster saturable absorption recovery, and more efficient pulse shaping, which all contribute to reducing the optical pulse width [1]. Beyond –5.5V SA biasing, the CPM operation began to be significantly affected by self-pulsation effects and mode locking could no longer take place. The minimal obtained pulse width in Fig. 3(b) was 1.7 ps occurred at 140 mA gain current during this optimization step.

In the last step, the DC and RF biasing parameters were further perturbed around the optimal condition extracted from Fig. 3 (a) and (b). Fig. 4(a) and (b) shows the final optimization results. The pulse width was nearly transform limited at 1.26 ps, with a spectral FWHM of 2.8 nm, for time-bandwidth product of 0.424. The biasing conditions were 25 dBm RF power at 14.085 GHz at 150mA gain current, -4.5V SA biasing. Fig.4(a) inset shows the 50 GHz scope trace of the CPM output triggered with RF source, showing good synchronization with minimal jitter. We see that selecting the appropriate DC and RF biasing conditions is critical for achieving the minimal pulse width for a given device design, which is important for using the synchronized CPM lasers as controlled ultrashort light sources in actual optical communication system applications.

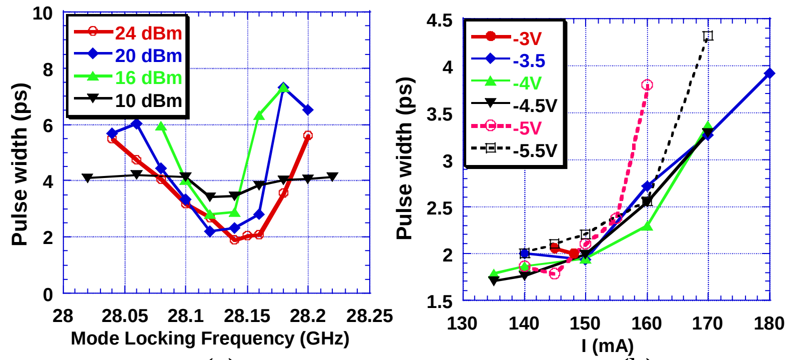

(a) (b)

Fig. 3(a) Autocorrelation pulse width of a 3000 μm CPM laser under second order SHML with (a) variation in RF modulation power and frequency (b) variation in DC SA biasing voltage and gain biasing current at 24 dBm, 14.075 GHz RF modulation (RF biasing condition for minimal pulse width in part (a)).

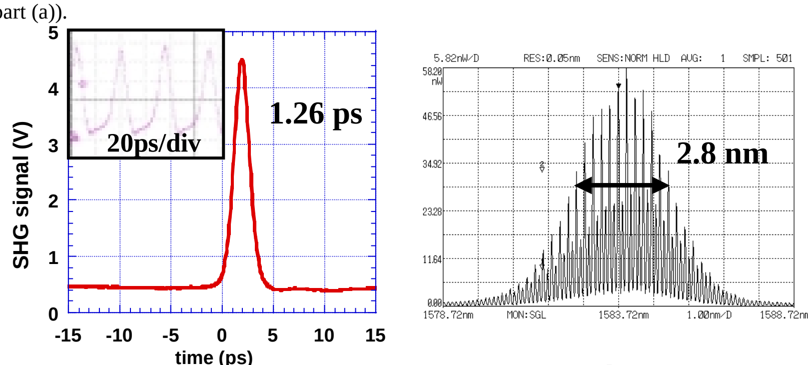

(a) (b)

Fig. 4(a) Autocorrelation trace of a 3000 μm CPM laser output under subharmonic hybrid mode locking. (a)Inset showing synchronized output on a 50 GHz sampling scope triggered with the RF source (b) corresponding optical spectrum.

For efficient optical pulse sharpening, the physical length of the saturable absorber should be shorter than the optical pulses [1]. The minimal pulse width of 1.26 psec achieved in Fig. 4(a) is comparable and limited by the transit time through the 50 μm saturable absorber plus the two 15 μm gaps (~0.93 ps). Further reduction in the SA dimension expected to provide shorter pulses and this investigation is currently underway.

4. Conclusion

In conclusion, we demonstrated electrical subharmonic hybrid mode locking operation at 28.2 GHz with the CPM laser BH waveguide fabricated through a deep RIE etching/MOVPE single step regrowth process. The CPM laser operated nearly transform-limited and well synchronized to external clock source with good phase stability. The pulse width was highly sensitive to RF and DC biasing conditions. After optimizations, a pulse width of 1.26 ps was achieved, limited by the saturable absorber dimension.

Reference:

[1] Y. K. Chen, M. C. Wu, "Monolithic colliding pulse mode-locked quantum well laser," IEEE J. Quantum Electron., vol. 28, pp. 2176-2185, Oct. 1992.
[2] H. K. Lee, V. Loyo-Maldonado, B. C. Qiu, K. L. Lee, C. Chu, S. Pinches, I. G. Thayne, A. C. Bryce, J. H. Marsh, "Efficient direct locking of colliding pulse mode-locked lasers on semi-insulating substrate at 1.5um," IEEE Photon. Technol. Lett., vol 14., pp1049-1051, Aug. 2002.
[3] T. Hoshida, H. F. Liu, M. Tsuchiya, Y. Ogawa, T. Kamiya, "Subharmonic hybrid mode-locking of a monolithic semiconductor laser," IEEE J. Select. Topics Quantum Electron., vol 2., pp514-522, Sept. 1996.
[4] S. Arahira, Y. Ogawa, "480-GHz subharmonic synchronous mode locking in a short-cavity colliding-pulse mode-locked laser diode," IEEE Photon. Technol. Lett., vol 14., pp537-539, April, 2002.
[5] C. Ji, R. G. Broeke, Y. Du, J. Cao, N. Chubun, P. Bjeletich, F. Olsson, S. Lourdudoss, R. Welty, C. Reinhardt, P. L. Stephan, S. J. B. Yoo, "Monolithically Integrated InP based Photonic Chip Development for O-CDMA Systems," IEEE J. Select. Topics Quantum Electron., to be published, Jan 2005.

This work was supported in part by DARPA/SPAWAR under agreement number N66001-02-1-8937, and by DARPA/ARO under agreement number W911NF-04-1-0066.